Quantification of the total suspended matter concentration in the sea breaking zone from *in situ* measurements and remotely sensed data – two empirical approaches

Ana C. Teodoro & André R.S. Marçal
University of Porto, Faculty of Science, Porto, Portugal; amteodor@fc.up.pt, andre.marcal@fc.up.pt

Fernando Veloso-Gomes
University of Porto, Faculty of Engineering, Porto, Portugal; vgomes@fe.up.pt

Keywords: TSM concentration, breaking zone, empirical relationships, image processing

ABSTRACT: Remote sensing techniques can be used to calculate suspended sediment concentrations and to understand the flux and distribution of sediments driven by mechanisms such as tides and waves, river discharges, etc.

The main objective of this study is the quantification of the Total Suspended Matter (TSM) concentration in the sea breaking zone for a particular area of the Portuguese coast, around Aveiro.

The methodology used was based on *in situ* measurements and multi spectral satellite images.

In situ experimental techniques (maritime platform, aerial platform, simulation on the beach and water sample collection in the breaking zone) were used to determine a relationship between the TSM concentration and the seawater reflectance in the breaking zone. Spectral reflectance was measured with a spectroradiometer and water samples were simultaneously collected. Empirical relationships were established between TSM concentration and the equivalent reflectance values for sensors SPOT/HRVIR, TERRA/ASTER and Landsat/TM at visible and Near Infra Red (NIR) bands computed from the experimental data.

Satellite images from ASTER, SPOT HRVIR and Landsat TM were used together with the same empirical models. These satellite images were calibrated and atmospherically corrected. Equations of linear, polynomial, logarithmic, power and exponential models were tested for the satellite image bands on the visible and near infrared. The coefficients of determination (R^2) were also calculated for each model.

The results obtained from the two approaches, *in situ* measurements and directly from the multi spectral satellite images, were analysed.

1 INTRODUCTION

There are a number of environmental applications for which the use of satellite data is essential, such as climatology and meteorology where the extensive size of the study areas would make any other source impractical. In the past few years there has been a fast development of the Earth observing platforms and sensors available for civil users.The successful development of a technique for monitoring coastal areas based on satellite data would enable us not only to keep an updated record of the coastal areas but also to obtain historical information that would be inexistent otherwise.

In coastal waters, the breaking zone is an area of great importance and very few studies have addressed this issue in the past, as there are obvious difficulties in getting data from this part of the coast. The successful development of a methodology to extract information about the breaking zone from satellite data would allow frequent updates and therefore enable us to implement an effective monitoring system.

Remote sensing techniques are valuable tools to obtain specific information on the spatial and temporal characteristics of the coastal zone. Substances in surface water can significantly change the characteristics of surface water reflectance. Remote sensing techniques depend on the ability to measure these changes in the spectral signature backscattered from water and relate these measured changes to a water quality parameter, such as suspended sediments (1), by empirical or analytical models.

The discrimination of suspended sediments or total suspended solids from water reflectance is based on the relationship between the scattering and absorption properties of water and its constituents. Most of the scattering is caused by suspended sediments and the absorption is controlled by chlorophyll-a and coloured dissolved organic matter. These absorptives in-water components have been shown to lower the reflectance in a substantial way. However, these absorptive effects are generally found at wavelengths less than 500 nm (2).

Various studies have been carried out combining *in situ* measurements and satellite data in order to relate spectral properties and water quality parameters. These studies developed empirical approaches to estimate the amount of suspended solid sediments (3) and used linear (4), polynomial, log-linear and log-log relationships between seawater reflectance and suspended sediment concentration (5). However, in none of these studies was it possible to establish a single algorithm to estimate the TSM concentration and its local variation. Moreover, these studies have been made for a specific place and for one determined date, not intending to estimate these relationships for other places and other times. These relationships become still more difficult when the aim is to study such a dynamic area as the breaking zone.

The objective of this study is the quantification of the TSM concentration in the sea breaking zone for a particular area of the Portuguese coast, around Aveiro, from *in situ* measurements and multispectral satellite data.

2 METHODS

Different *in situ* techniques (maritime platform, aerial platform, simulation on the beach and water sample collection in the breaking zone) were used to determine a relationship between the TSM concentration and the spectral response of the seawater. These relationships were used to directly obtain the TSM concentration from the reflectance of the multispectal satellite data tested.

2.1 *Study area*

A part of the northwest coast of Portugal, around Aveiro, was chosen as a test area. This area is limited to the north by the Douro River mouth and to the south by Mira Lagoon (Figure 1). The total extension of this area is about 80 kilometers with an orientation NNE-SSE.

The littoral drift current acts principally in the north-south direction. The wave climate has medium significance with wave heights from 2 to 3 meters, with periods ranging from 8 to 12 seconds. Tides are of semidiurnal type, reaching a range of 2 to 4 meters for spring tides. Meteorological tides are not significant.

The causes of the present situation of generalised coastal erosion, in this particular area, have been identified as a coastal response to the weakening of the river basin sediment sources and river sediment transport, the mean sea level rise, the human occupation of waterfront and dune destruction (6). The hydroelectric plants reduce drastically the volume of solids transported to the the sea. The reduction of sediment transport is also associated with the extraction and dredging of sand rivers and with the river flow evolution along the year.

2.2 *Field work*

A fieldspec spectroradiometer was used in all the field work techniques to determine the sewater reflectance. This optical sensor operates between 350 and 2,500 nanometers and has a spectral resolution of 10 nanometers. The data collection is made through a fiber optic cable input with 1.2

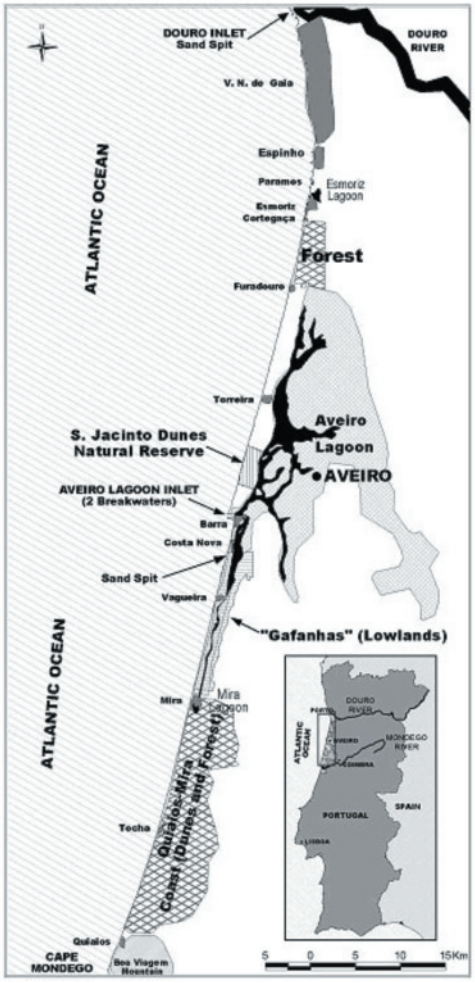

Figure 1. Study area between the mouth of the River Douro and Mira Lagoon.

meters in length and a 25 degrees full angle cone field-of-view. The data quality critically depends on the precision at the calibration stage.

The quantification of the TSM (milligram per liter) of each water sample collected was made through a standard filtering process. The 1 liter water samples collected were refrigerated in the dark and processed after a few hours in the chemistry laboratory. A cellulose nitrate filter was used, with a diameter pore of 0.45 micrometers. The quantification of TSM was made subtracting the final and the initial weight of the filters.

The purpose of the field campaigns using boats was to simultaneously collect water samples and measure the seawater reflectance. The first two campaigns were scheduled so that they would coincide with clear-sky satellite overpasses by ASTER, but unfortunately, atmospheric conditions invalidated the image acquisition. In the third campaign, a boat from the Portuguese marine institute was used on 10 July 2003 to collect water samples and simultaneously measure the reflectance, as shown in Figure 2(a). The position and depth of each location were also measured using a Global Positioning System (GPS) receiver and an echo-sounding lead. The TSM concentrations and the reflectance values were very similar for the 3 levels of TSM tested, as can be seen in Figure 2(b).

However, it was obviously difficult to collect data close to the breaking zone, as it was impossible to immobilize the boat. A more stable platform was therefore required. Helicopters provide an efficient platform for the collection of water samples and for reflectance measurements for several reasons. Firstly, a large area can be sampled rapidly and secondly, the platform can be immobilized over the sea breaking zone.The helicopter was stabilized about 2-3 meters above the sea surface and

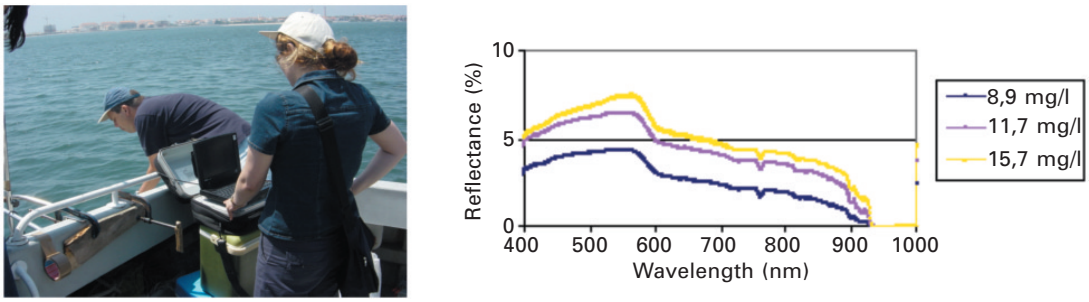

Figure 2. Boat used in the field work (a) and TSM concentration vs. Reflectance (b).

30 samples of water were collected and the reflectance measured simultaneously. The position of the helicopter was identified using a GPS receiver.

In order to simulate different concentrations of suspended sediments, several field campaigns were carried out on different beaches of the study area. The sediment type was found to be very similar in the whole study area. A container 0.8 meters high and 0.4 meters in diameter was used (Figure 3 (a)). To minimize the effect of reflection from the sides and bottom of the container, it was lined with a black and completely opaque plastic. The reflectance was measured and water samples (mixed) were taken simultaneously for a range of sediment concentrations. The container conditions caused a signal attenuation in the reflectance values. This attenuation was quantified through some measures of the seawater sample reflectance carried out inside the container and also with a wet sand background. The relationship between container and wet sand background was found to be nearly constant for all concentrations of TSM tested. Figure 3(b) shows a typical example of this attenuation, in this case for a TSM concentration of 30 milligram per liter.

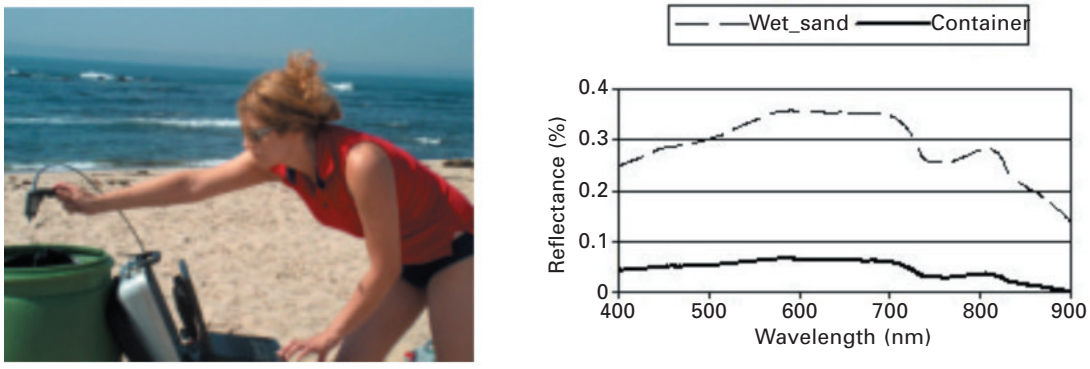

Figure 3. Simulations on the beach (a) and signal attenuation (b).

The reflectance values had very high correlation with the TSM concentration at the wavelengths between 500 and 900 nanometers. There is a peak in reflectance between 550 and 600 nanometers, and above 900 nanometers the reflectance is practically zero for lowest reflectances (Figure 4).

As it was almost impossible to obtain water samples and simultaneous radiometric measurements in the breaking zone, an evaluation of the range of TSM values typically found in this area was undertaken. To get water samples directly from the breaking zone and the swash zone, a surfboarder was hired to collect water samples in small transparent containers, as can be seen in Figure 5(a). The reflectance was measured for each water sample collected by putting the transparent small container (about 1 liter each) in the wet sand trying to simulate the sea bottom conditions. The average value of TSM concentration found in the breaking zone was 32 milligram per liter and in the swash zone 50 milligram per liter. The average reflectance values for these two areas are very similar, as shown in Figure 5(b).

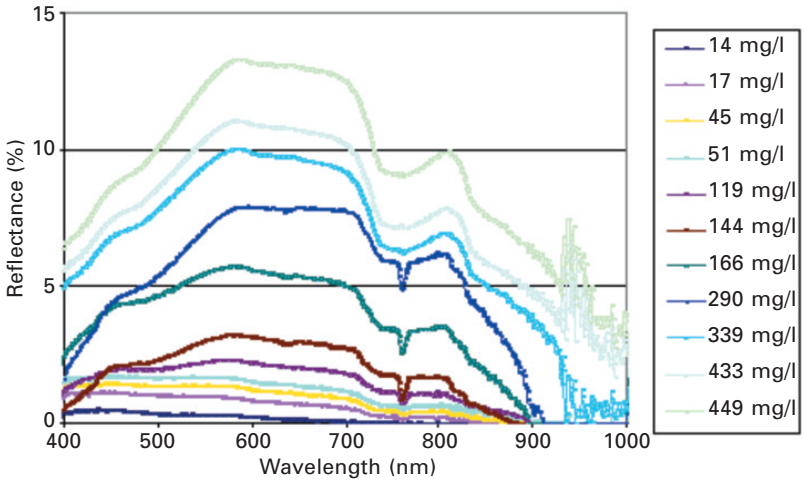

Figure 4. Relationship between TSM concentration and seawater reflectance.

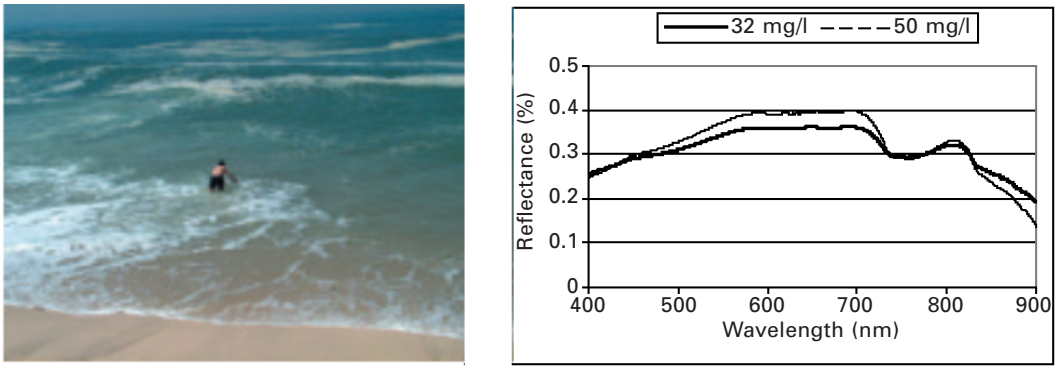

Figure 5. Surfboarder in the swash zone (a) and TSM concentration for two water samples (b).

3 RESULTS

3.1 *Establishment of Empirical Models*

Based on *in situ* measurements of TSM concentration and sea water reflectance, empirical models were established to relate them to each other. The water-leaving equivalent reflectance (R_{ES}) for each sensor band in the visible and NIR was calculated by equation (1), where R_m is the reflectance measured by the spectroradiometer, ϕ is the sensor spectral normalized response and λ is the wavelength.

$$R_{ES} = \frac{\int R_m(\lambda)\phi(\lambda)d\lambda}{\int \phi(\lambda)d\lambda} \quad (1)$$

A relationship between seawater reflectance and the TSM concentration was established for each band of Landsat TM, ASTER, and SPOT HRVIR. Equations of linear, polynomial, logarithmic, power and exponential models were tested for all satellite image bands, as presented in Table 1.

The coefficients of determination (R^2) were also calculated for each model. For the visible and NIR bands of Landsat TM the linear and polynomial models tested presented a high determination coefficient ($R^2 \geq 0.96$). The results were slightly worse for power and exponential models, as presented in Table 2.

Table 1. Empirical models established

Model	Equation
Linear	$R = A*TSM + B$
Polynomial	$R = A*TSM^2 + B*TSM + C$
Logarithmic	$R = A*\log_{10}(TSM) + B$
Power	$R = A*TSM^B$
Exponential	$R = Ae^{B*TSM}$

Table 2. Regression coefficients of reflectance functions vs TSM concentration for TM data

Bands	Linear			Polynomial				Power			Exponential		
	A	B	R^2	A	B	C	R^2	A	B	R^2	A	B	R^2
TM1	0.02	0.37	0.96	$0.06E^{-4}$	0.02	0.53	0.96	0.07	0.76	0.92	0.97	0.01	0.84
TM2	0.03	0.09	0.97	$0.01E^{-4}$	0.03	–0.12	0.97	0.04	0.93	0.94	0.90	0.01	0.82
TM3	0.03	–0.13	0.97	$0.03E^{-5}$	0.03	0.12	0.97	0.02	1.05	0.94	0.71	0.01	0.79
TM4	0.02	–0.63	0.96	$0.01E^{-3}$	0.01	–0.28	0.97	$0.05E^{-2}$	1.62	0.90	0.12	0.01	0.70

The results obtained for SPOT HRVIR for all models tested are comparable to those obtained with TM data. As an illustration of the results obtained for SPOT HRVIR, Figure 6(a) shows a graphical representation of the linear model for band XS1 of SPOT.

The coefficient of determination for all models established for ASTER VNIR bands follows the same pattern as those obtained for SPOT HRVIR and TM data. As an example, Figure 6(b) shows a graphical representation of the exponential model for band VNIR1 of ASTER.

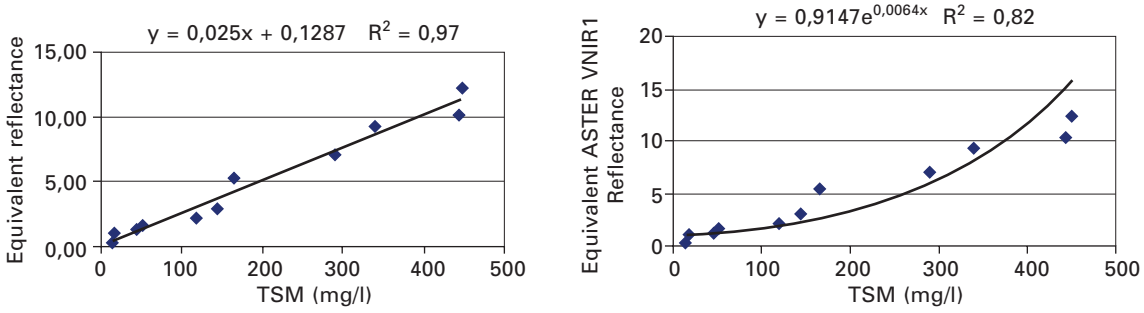

Figure 6. (a) Linear model for SPOT XS1 and Exponential model for ASTER VNIR1 (b).

The linear models established for all the images tested present a determination factor (R^2) higher than 0.95. The non-linear models present a lower but acceptable coefficient of determination factor. A great similarity was verified between the coefficients model and determination factors for spectrally comparable bands on different sensors. This indicates that the small variations in the band widths of the different sensors tested did not affect the model coefficients. These parameters are presented in Table 3 for the green bands of ASTER, TM and HRVIR sensors.

Table 3. Coefficient model for identical bands of SPOT, ASTER and TM

Sensor/Band	Wavelength (nm)	A	B	R^2
SPOT/XS1	500–590	0.025	0.128	0.97
ASTER/VNIR1	520–600	0.025	0.131	0.97
Landsat/TM1	520–600	0.026	0.088	0.97

3.2 *Multi Spectral Satellite Data*

A group of satellite images were acquired, five from Landsat TM, two from ASTER and one from SPOT HRVIR. These images are all cloud-free for the study area. The image acquisition date and the corresponding time and tide heights are presented in Table 4.

Table 4. Acquisition parameters of the images used

Satellite Sensor	Date	Acquisition Time (UT)	Tide Height (m)
Landsat TM	9 November 1989	10:45	2.95
Landsat TM	4 May 1990	10:45	2.33
Landsat TM	1 November 1992	10:45	1.85
Landsat TM	13 June 1993	10:45	2.47
Landsat TM	24 July 1997	10:45	1.09
SPOT HRVIR	14 October 1998	11:35	2.85
TERRA ASTER	8 October 2001	11:43	1.29
TERRA ASTER	24 October 2001	11:43	2.07

In order to directly obtain the TSM concentration from the reflectance of the satellite images, all satellite image bands from visible and NIR were calibrated for radiance values, using equation (2):

$$L_i = \alpha_i DN_i + \beta_i \tag{2}$$

where L_i is the spectral radiance ($Wm^{-2}\ sr^{-1}\ \mu m^{-1}$), DN_i is the digital number, α_i and β_i are the calibration coefficients for the spectral band *i* of a given sensor. The calibration coefficients used are listed in Table 5.

Table 5. Radiance calibration coefficients for visible and NIR bands of all images acquired

Sensor	Band 1		Band 2		Band 3		Band 4	
	Slope (α)	Offset (β)	Slope (α)	Offset (β)	Slope (α)	Offset (β)	Slope (α)	Offset (β)
ASTER	0.676000	–0.676000	0.708000	–0.708000	0.862000	–0.862000	–	–
SPOT HRVIR	2.58326	0	3.30575	0	2.01466	0	–	–
Landsat TM	0.602431	–1.52	1.1751	–2.52	0.805765	–1.17	0.814549	–1.51

The reflectance (R_i) values for all satellite image bands were obtained using equation (3).

$$R_i = \frac{\pi L_i d^2}{E_i \cos\theta} \tag{3}$$

where L_i is the spectral radiance and E_i is the mean solar exoatmospheric irradiances for the spectral band i; d is the Earth-Sun distance in astronomical units and θ is the solar zenith angle in degrees.

The satellite images must be atmospherically corrected adequately before further analysis. Atmospheric effeb(are critical factors, particularly because the water-leaving radiance detected by the sensor is very low with respect to the contribution of the atmospheric path radiance. These effects are wavelength-dependent. The objective of atmospheric correction is the retrieval of the ground surface spectral reflectance from the top of the atmosphere radiance measured at the sensor. When *in situ* measurements (atmospheric model for gaseous components, aerosol model, etc.) are

not available, information about atmospheric properties could be derived directly from the image. Image-based methods are less accurate than radiative transfer models, but constitute a valid alternative when atmospheric properties are not measured during the image acquisition. The Dark Object Subtraction (DOS) method assumes that atmospheric path radiance is the radiance value measured by the satellite for the darkest object within the image, usually clear water bodies or areas in complete shadow (7). This model corrects only the atmospheric additive scattering component. The Improved DOS method uses a relative atmospheric scattering model to consider the multiplicative efects. Therefore, the atmospheric correction procedure was based on an Improved DOS technique. The spectral band histograms were analysed and selected a start band DOS haze value. After a relative scattering model had been chosen based on the atmospheric conditions of the image at the acquisition time the initial haze value for the others spectral bands was calculated. The DN value that will be subtracted for each band was calculated after normalization, using equation (4):

$$DN\ (HAZE_i) = NORM_i * HAZE_i + OFFSET_i \quad (4)$$

where DN ($HAZE_i$) is the DN value that predicted $HAZE_i$ value will be mapped in band *i*, $NORM_i$ is the normalized gain value, $HAZE_i$ is the predicted haze value for band *i* using a relative scatterring model and the offset corrected starting haze value, and $OFFSET_i$ is the offset value used for band *i*.

The empirical models established based on *in situ* measurements were applied for real satellite data. A single application example of a linear model (Table 6) for an ASTER image (24/10/2001) is presented here.

Table 6. Linear model coefficients for an ASTER image ($TSM_{(VNIR1)} = A*R_{(VNIR1)} + B$)

Band	A	B	R^2
$VNIR_1$	38.334	0.4135	0.97
$VNIR_2$	35.837	12.209	0.97
$VNIR_3$	50.266	36.271	0.97

Figure 7 presents the TSM concentration for the study area estimated from each of the 3 bands (visible and NIR) of the ASTER image.

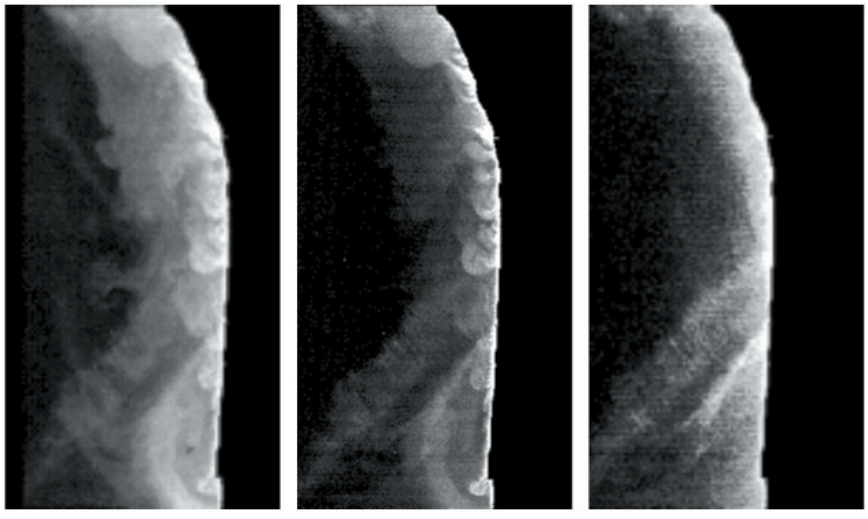

Figure 7. Application of the linear model to an ASTER image ($VNIR_1$, $VNIR_2$, $VNIR_3$).

Different sedimentary patterns and areas with TSM concentration variations are better visible in Figure 8.

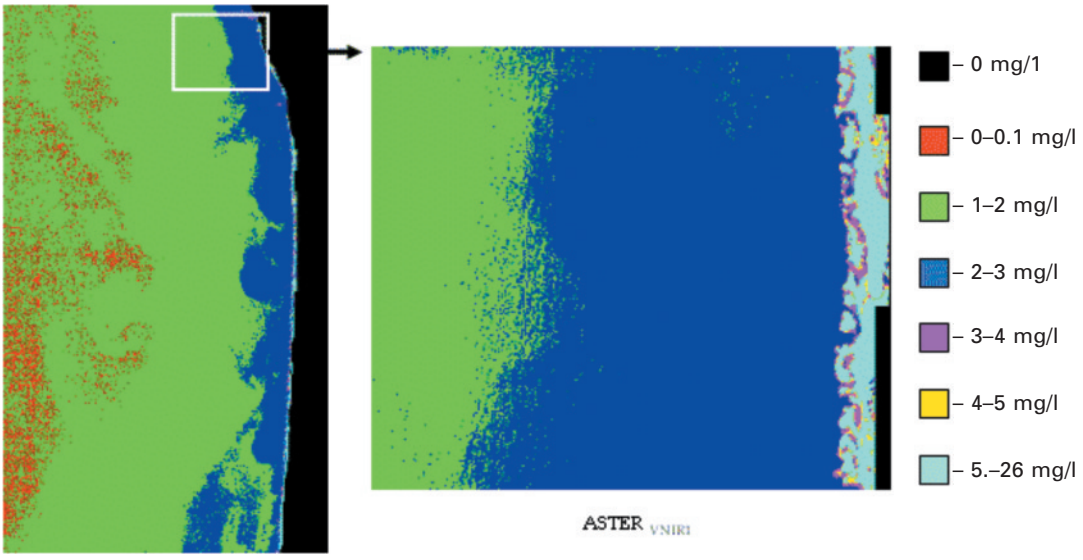

Figure 8. Application of the linear model to an ASTER image ($VNIR_3$): graduated colour legend.

4 CONCLUSIONS

This study shows that multispectral satellite images can be used to obtain the TSM concentration in the sea breaking zone. As an illustration, an empirical model was applied to one ASTER image. The results are very promising and the same methodology is currently being applied to SPOT HRVIR and Landsat TM images. The calibration and the atmospheric correction precision were essential to obtain a more effective relationship between the seawater reflectance and the TSM concentration.

The measurement conditions affect the results. The influence of sea bottom and open ocean in the reflectance measures and the distribution of the sediments in the water column need to be considered. The different measurement conditions were investigated to address this issue. The container aimed to simulate the deep sea conditions, without the sea bottom influence, and the measures made with the wet sand background attempted to simulate the sea bottom influence. However, the *in situ* measurements proved important to calibrate the process in order to establish the empirical relationships between TSM concentration and seawater reflectance for each sensor/band.

ACKNOWLEDGEMENTS

This work was done within the COSAT (COastal zones monitoring using remote sensing SATellite data) project, financed by the Portuguese Science and Technology Foundation (FCT) through the POCTI/FEDER program.

REFERENCES

1. Ritchie, J.C., Zimba, P.V. & Everitt, J.H., 2003. Remote sensing Techniques to Acess Water Quality, *Photogrammetric Engineering & Remote Sensing*, Vol. 69, No. 6: 695-704.
2. Myint, S.W. & Walker, N.D., 2002. Quantification of suspend sediments from satellite, *International Journal of Remote Sensing*, Vol. 23, No. 16: 3219-3249.

3. Ritchie, J.C., McHenry, J.R., Schiebe, F.R. & Wilson, R.B., 1974. The relationship of reflected solar radiation and the concentration of sediment in the surface water of reservoirs, *Remote Sensing of Earth Resources*, Vol. III: 57-72
4. Islam, M.R., Begun, S.F., Yamaguchi, Y. & Ogawa, K., 2001. Suspend sediments in the the Ganges and Brahmaputra Rivers in Bangladesh: Observation from TM and AVHRR data, *Hydrological Processes*, Vol. 15: 493-509
5. Forget, P. & Ouillon, S., 1998. Surface suspend matter off the Rhone river mouth from visible satellite imagery, *Oceanologica Acta*, Volume 21, No. 6: 739-749.
6. Veloso-Gomes, F., Taveira-Pinto, F., Barbosa, J.P., Neves, L. & Coelho, C., 2002. High risk situation in the NW Portuguese coast: Douro River – Cape Mondego. In: *Proceedings of Littoral 2002, The Changing Coast*, Edited by EUROCOAST/EUCC, 411-421.
7. Chavez, P.S., 1988. An improved Dark Object Subtraction technique for atmospheric scattering correction of multispectral data, *Remote Sensing of Environment*, No. 24, 459-479.